ISSN NO. 2320-5407

Journal homepage:http://www.journalijar.com

INTERNATIONAL JOURNAL OF ADVANCED RESEARCH

RESEARCH ARTICLE

Dipron: an eco-friendly corrosion inhibitor for iron in HCl media in both micro and nano scale particle size - Comparative study.

Enas Mohamed Attia.
Chemistry Department, Faculty of Science (Girls), AL-Azhar University, Nasr City, Cairo, Egypt.

Manuscript Info

Manuscript History:

Received: 14 January 2016
Final Accepted: 26 February 2016
Published Online: March 2016

Key words:
Corrosion, Inhibition, Adsorption, Microscale, Nanoscale, Sulfa drug

****Corresponding Author***

Enas Mohamed Attia.

Abstract

This study was performed in order to investigate the ability of using sulfa drug (Dipron) with heterogeneous particle size in both micro and nano scale forms as an eco-friendlycorrosion inhibitor for iron (Fe) in hydrochloric acid solutions, in addition to decide which form would be more effective to inhibit Fe corrosion. The particle size analysis for micro and nano scale of Dipron was determined using BT-2001(Liquid) laser particle size analyzer and dynamic light scattering (DLS) respectively. Open circuit potential measurements, potentiodynamic and potentiostatic polarization techniques were performed at temperature range 20–60 °C. The outcomes showed that inhibition took place by adsorption of the Dipron on Fe surface without altering the mechanism of corrosion process. The adsorption of Dipron on Fe surface was consistent with Langmuir's adsorption isotherm. Physical adsorption mechanism was proposed from the calculated activation energy and thermodynamic parameters for the two forms of Dipron. The negative values of free energy of adsorption (ΔG°_{ads}) indicated that adsorption of Dipron followed a spontaneous process. The obtained results indicated that nano- scale of Dipron (NSD) has higher efficiency for corrosion inhibition than micro scale of Dipron (MSD). The inhibition efficiency increased with a corresponding increase in the inhibitor's concentration and decreased with rise of temperature.

Introduction:-

Fe has a significant impact on our day– to– day life, directly or indirectly. The main reason behind large scale usage of this metal is that it is not very expensive as compared to other metals, and is also abundantly available on the surface of the earth. This metal, which is the most commonly used, corrodes in many media especially acidic one. The application of acid corrosion inhibitors in the industry is widely used to prevent or minimize material loss during contact with acid (Selvakumar*et al*., 2013). Most of organic compounds which are largely used as corrosion inhibitors are toxic in nature. This revealed the need of environmentally friendly inhibitors. Recently, there is a growing interest on the development of drugs as inhibitors for metallic corrosion due to their non-toxic nature (Quraishi*et al*., 2012). The choice of drugs used as corrosion inhibitors is based on the following facts: (a) the molecules have oxygen, nitrogen and sulphur as active centers, (b) they are healthy i.e. not hazardous and environmentally friendly and (c) they can be easily produced and purified (Ebenso *et al*., 2009).Sulphonamides are drugs extensively used for the treatment of infections caused by gram-positive microorganisms, some fungi, and certain protozoa. Other therapeutic uses of sulfonamides are as diuretic and hypoglycemic agents (Arslan *et al*., 2009). Dipron, which is one of the simplest sulphonamides, hasnumbers of functionaladsorption centers (e.g. –NH_2 group,–SO_2–NH– group and aromatic ring). It is strongly basic hence it can be readily soluble in the acid medium.

In view of the above, the aims of the present work are: (1) to make a comparative study on the inhibition of Fe corrosion in HCl solution by Dipron in both micro and nano scale forms using electrochemical methods. (2) to study the effect of temperature and concentration on the inhibitive properties of the drug in its two particle size scales. (3)

to study the adsorption characteristics of the drug in its two scales by fitting the adsorption data into different adsorption models.

Materials and Methods:-

Specimen's preparation:-

The specimen of Fe (99.99% purity, Alfa Ventron)with 1.643 cm^2 exposed area was made of massive cylindrical rod mounted into glass tube by epoxy resin. A copper wire was employed for an electrical contact. Before each experiment, the Fe surface was polished mechanically using emery papers of Grade Nos. 220, 400, 600, 800 and 1200 until its surface became smooth and mirror-like bright, then it was cleaned by washing thoroughly with distilled water and finally degreased with acetone.

Solutions and inhibitor:-

The aggressive solution was prepared by dilution of AR grade 37% HCl in bi-distilled water. The acidconcentrations (0.05, 0.10, 0.25, 0.50, 0.75, 1.00 and 2.00 M) were prepared at 25 °C.

The sulfa drug (Dipron),4-(Aminosulfonyl)aniline, is of AR grade purchased from Nile Company for Pharmaceuticals and Chemical Industries and used as inhibitor without further purification. Its molecular weight is 172.2 g/mol with melting point and density 165 °C and 1.08 g/cm^3, respectively. The chemical structure of Dipron is represented in Figure 1. The particle size of the purchased Dipron was determined using a high performance BT-2001(Liquid) laser particle size analyzer. Figure 2 represents the relation between diffraction and accumulation of Dipron molecules with its size.

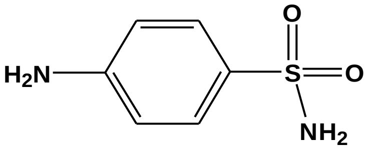

Fig 1: Chemical structure of Dipron: (4-(Aminosulfonyl)aniline)

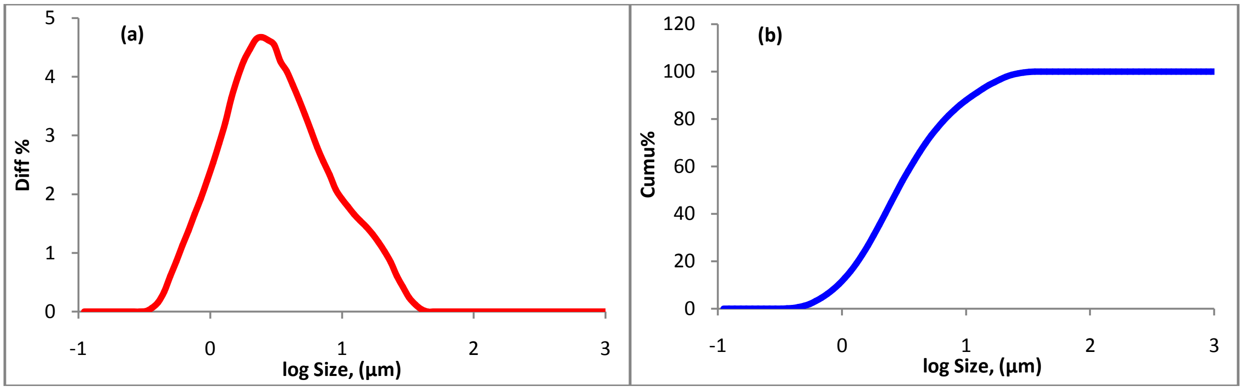

Fig 2: Relation between particle size with (a) diffraction and (b) accumulation of molecules.

The particle size analysis illustrated that the different percentages of particles with its different micro size are as follows: D3: 0.607 µm, D6: 0.754 µm, D10: 0.931 µm, D16: 1.182 µm, D25: 1.550 µm, D50: 2.811 µm, D75: 5.607 µm, D84: 8.160 µm, D90: 11.40 µm, D97: 19.55 µm and D98: 21.87 µm with medium index =1.00. On the other hand the percent of each present specified size in the system medium is illustrated in Table 1. Figure 2 and Table 1 illustrated the heterogeneity of the system which all falls in the micro scale level. Thus purchased micro scale ofDipron can be referred as MSD.

Table 1: Relation between particle size and its percentage in the medium

Size(µm)	0.323	0.548	0.929	1.576	2.674	4.537	7.698	13.060	22.160	37.670
Percent	0.00	1.94	9.94	25.62	47.88	68.38	82.74	92.06	98.10	100.00

The nano scale of Dipron (NSD) was prepared by grinding MSD using ball mill at 200 rpm for 10 hours. The particle size of NSD was determined using dynamic light scattering (DLS). As can be seen from Figure (3), in number distribution technique, there is only one peak of 100% particle sizes equal to 159.4 nm. The polydispersity index value (PDI = 0.364) reflected the slightly mono-disperse in size and indicated that the sample had a relatively narrow size distribution with width equal to 89.68 nm.

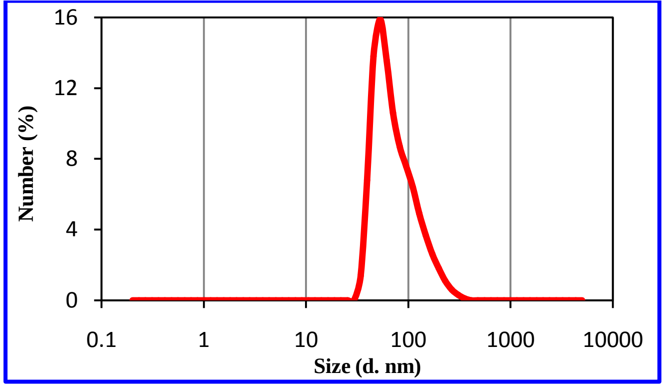

Fig 3: Size distributions of NSD by number.

Different concentrations of Dipron (0.19, 0.95, 1.90, 3.80, 9.50, 10.00 and 13.31 mM) were prepared at 25°C by dissolving a calculated amount of the inhibitor in 0.5M HCl.

Electrochemical techniques:-

Open circuit potential measurements:-

Open circuit potential (OCP) measurements were carried out in a double- walled glass cell filled with 25 ml of the test solution. The potentials were measured with the aid of digital multimeter (KEITHLEY, Model 175, USA) using saturated calomel electrode (SCE) as a reference electrode.

Potentiodynamic polarization:-

In potentiodynamic polarization technique, measurements were performed by changing the electrode potential from negative to positive direction at scan rate 3mV/s. The corrosion rate (C_R) in mpywas calculated using Eq.1 (Pathak, 2013):

$$C_R = 0.13 \times I_{corr} \times e/\rho (1)$$

where 0.13 is the metric and time conversion factor,I_{corr}, is the corrosion current density in μA/cm^2, e is the equivalent weight of metal in geq/mol andρ, is the density in g/cm^3. Values of I_{corr} and corrosion potential (E_{corr}) were determined from the extrapolation of linear Tafel segments of anodic and cathodic curves. The inhibition efficiency (IE%) was evaluated from the measured I_{corr} values using Eq.2:

$$IE\% = \left[1 - \frac{I_{corr}}{I^{\circ}_{corr}}\right] \times 100 \ (2)$$

whereI°_{corr} and I_{corr} are the corrosion current densities in absence and presence of inhibitor, respectively.

Potentiostatic polarization:-

In potentiostatic polarization, the experiments were undertaken by applying a constant voltage values (-150, -100, +10, +50, +100 and +200 mV(SCE)) to the working Fe electrode immersed in 0.5M HCl in absence and presence of Dipron in each of MSD and NSD forms and the corresponding current densities were recorded as a function of time.

The quantity of electricity (Q) passed through the metal surface was calculated from the relation $Q = It$, where I is the current density recoded corresponding to the applied voltage at time t. The surface charging capacity (C) was calculated from Eq. 3:

$$C = Q/V \qquad (3)$$

where$V$ is the constant voltage applied across the metal surface. The reciprocal capacitance (C^{-1}) was in proportion to the thickness of the oxide film (d) according to Eq. 4 (Attia, 2015):

$$d = \varepsilon\varepsilon^{\circ} A C^{-1} \qquad (4)$$

where$A$ is the electrode surface area, ε is the dielectric constant of oxide and $\varepsilon^{\circ}$is the permittivity of free space ($8.845 \times 10^{-14}\ F/cm$).

Potentiodynamic and potentiostatic polarization measurements were generated using a Wenking Electronic Potentioscan (Mode l73) with the aid of a saturated calomel electrode (SCE) and platinum sheet (4 cm^2) as a reference and counter electrodes respectively. The indicated results are the mean of four experiments.

Results and Discussion:-

Open circuit potential measurements:-

Effect of different concentrations of Dipron on OCP of Fe electrode:-

Figure 4 illustrated the OCP of Fe immersed in 0.5M HCl in absence and presence of different concentrations (0.19 -13.31 mM) of Dipron. The electrode potential shifted to more passive values in presence of Dipron inMSD and NSD forms compared with that of free HCl solution, indicating the inhibiting action of Dipron in its two forms. Considering the lowest (0.19 mM) and the highest (13.31mM) Dipron concentrations, the steady state potential (E_{ss}) was ranging from -353 to -337 mV(SCE) in presence of MSD and from -353 to -308 mV(SCE) in presence of NSD after 120 minute of immersion (E_{ss} of Fe in free 0.5M HCl = -360 mV(SCE)). This means that at the studied concentrations, NSD shifted the electrode potentials to positive values more than MSD, indicating better effect on corrosion inhibition process in 0.5M HCl. These results indicated that in OCP measurements, Dipron in both MSD and NSD forms stimulated the corrosion inhibition process in 0.5M HCl and the effect of NSD was more pronounced than MSD. On the other hand, 10 mMDipron concentration represented an odd behavior where its E_{ss} values are -290 and -302 mV(SCE) for MSD and NSD respectively. These values exceeded that corresponding to the highest Dipron concentration (13.31 mM). Thus, 10 mM represented an optimum concentration for corrosion inhibition process in OCP measurements.

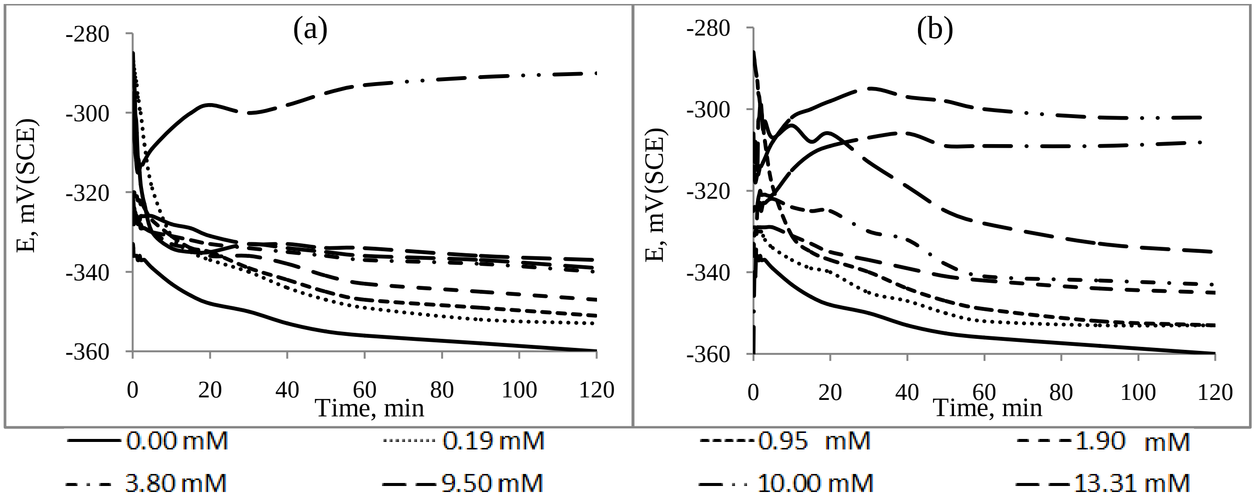

Fig 4: Effect of Dipron concentrations on OCP of Fe in 0.5M HCl: (a) MSD, (b) NSD.

Effect of different concentrations of HCl in absence and presence of 10 mM of Dipron on Fe electrode:-

The potentials of Fe electrode immersed in different concentrations (0.05-2.00 M) of HClin absence and presence ofDipron (10 mM) were measured as a function of immersion time as shown in Figure 5. The potentials of Fe electrode in free HCl (Figure 5a) tended towards more negative potential represented the breakdown of the pre-immersion air formed oxide film presented on the surface according to Eq.5 (Abdel Hameed, 2011):

$Fe_2O_3 + 6HCl \rightarrow 2FeCl_3 + 3H_2O$ (5)

The general shift, to noble direction, points to oxidation of Fe_3O_4 to Fe_2O_3 according to Eq.6 (Pourbaix, 1974).

$4Fe_3O_4 + O_2 \rightarrow 6Fe_2O_3$ (6)

Figure 5(b and c) indicated that addition of Dipron (10 mM) in MSD and NSD forms to the medium produced a slight positive shift in the open circuit potential due to the retardation of the anodic reaction.

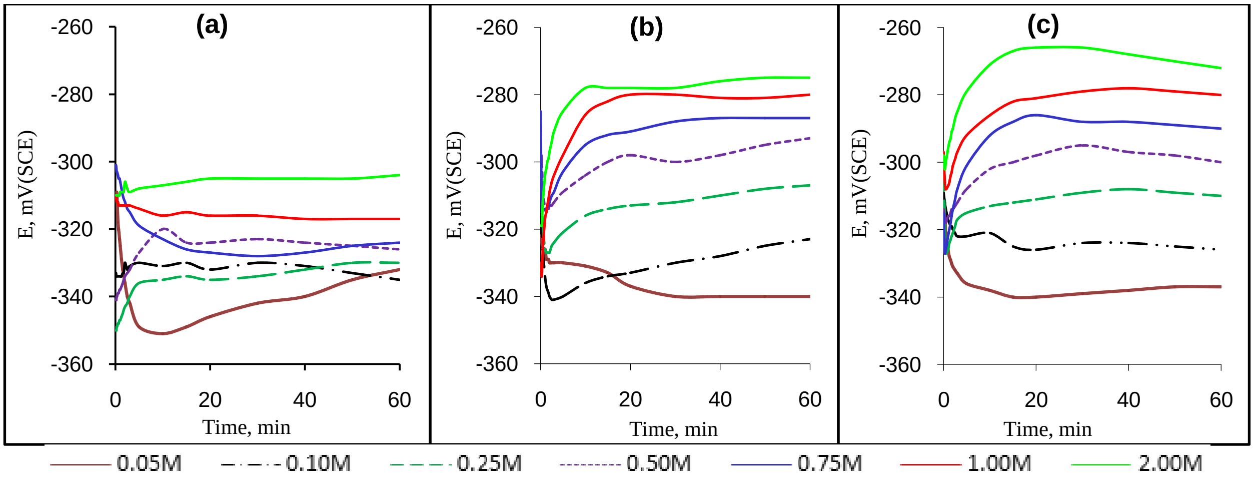

Fig 5: Potential – time curves of Fe in different concentrations of HCl in absence and presence of 10 mM of Dipron: (a) Free HCl (b) MSD (c) NSD.

The variation of E_{ss} with the logarithm of the molar concentration, C, of the acid solutions, was represented inFigure 6. The results revealed that E_{ss}varied linearly with $\log C$ according to Eq. 7:

$$E_{ss} = \alpha + b \log C \qquad (7)$$

where, α represents the steady state potential in solution of 1 M concentration, and b is the slope of the straight line. The constants α and b are depending on the composition of solution. Values of $\alpha$and b for Fe in free HCl were equal to -316 mV(SCE) and 20 mV per decade concentration respectively. Addition of 10 mM of Dipron in MSD and NSD forms shifted the steady state potentials positively with extrapolated values of α were -284 and -283 mV(SCE) and values of $b$were 41 and 38 mV per decade concentration, respectively. These values indicated that 10 mM of Dipron in MSD and NSD forms had similar inhibiting effect on open circuit potential of Fe in different concentrations of HCl solutions with preferential action of NSD form.

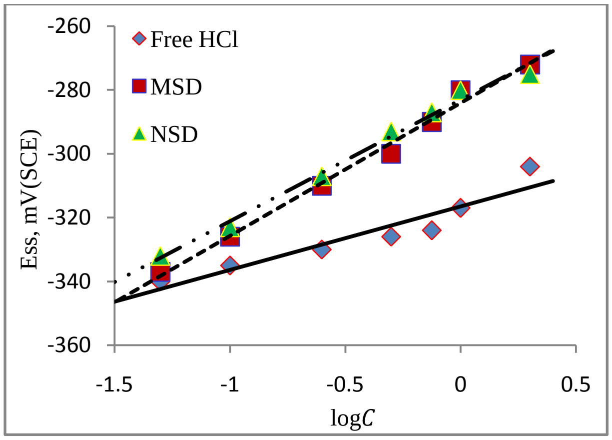

Fig 6: E_{ss}vs. $\log C$ for Fe in different concentrations of HCl solutions in absence and presence of 10 mM of Dipron in MSD and NSD forms.

Potentiodynamic polarization measurements:-

Effect of HCl concentrations on corrosion behavior of Fe electrode:-

Polarization plots of Fe in different concentrations of HCl (0.05 - 2.00 M) at 25 °C are shown in Figure 7. The respective potentiodynamic parameters including corrosion potential (E_{corr}), corrosion current density (I_{corr}), corrosion rate (C_R), anodic (b_a) and cathodic(b_c) Tafel slopes were listed in Table 2.

The analysis of the data in Table 2 revealed thatI_{corr} and $C_R$increased with increasing acid concentration. This indicated that the aggressive Cl^- ions participated in the dissolution process. The Fe metal was oxidized at the anode where corrosion occurs according to Eq. 8:

$Fe = Fe^{+2} + 2e^{-}$ (8)
Simultaneously, reduction occurs at cathodic sites according to Eq. 9:
$2H^{+} + 2e^{-} = H_2$ (9)
Chloride ions typically migrated into Fe from the environment and, upon reaching embedded Fe and exceeding a certain critical concentration, destroyed the passivating oxide layer on Fe forming complexes with ferrous ion. This led to formation of expansive corrosion products. Some of these products are soluble and assist transport of corrosion products away from sites where they might otherwise gave physical protection (Balonis, 2010). This corrosion process can be suppressed by using an appropriate dose of inhibitor, which reacted with and complex ferrous ions, or adsorbed on its surface thus interrupting the corrosion process.

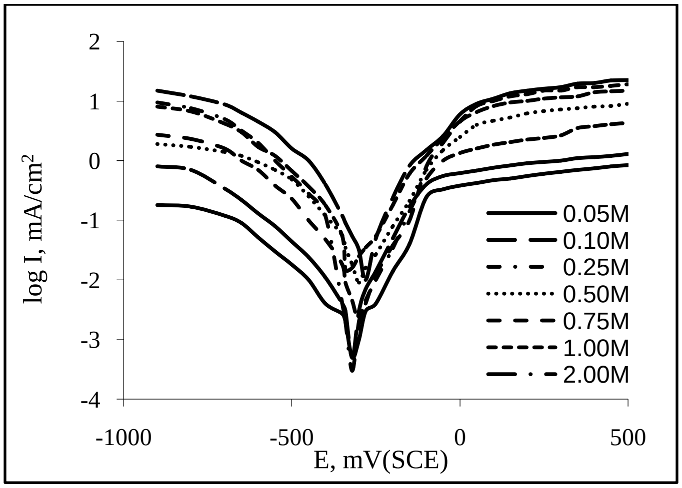

Fig 7: Potentiodynamic polarization plots of Fe in different concentrations of free HCl solutions.

Table 2:Potentiodynamicparameters of Fe in different concentrations of free HCl

C_{HCl} M	E_{corr} mV(SCE)	I_{corr} μA/cm^2	C_R mpy	b_a mV/dec	- b_c mV/dec
0.05	-320	100	46	100	200
0.10	-320	355	164	214	167
0.25	-320	950	439	94	36
0.50	-300	970	448	111	143
0.75	-300	1400	647	91	143
1.00	-340	1995	921	100	200
2.00	-280	2512	1160	91	100

Effect of HCl concentrations on the inhibition efficiency of 10 mM of Dipron using Fe electrode

The effect of changing HCl concentrations on the inhibition efficiency of 10 mMDipron was demonstrated in Figure 8 and the corresponding potentiodynamic parameters are represented in Table 3. It could be seen that, with increasing acid concentration and in the presence of Dipron (10 mM), the anodic and cathodicTafel slopes changed greatly from that of free acid solutions (Table 2). This showed that addition of 10 mM of Dipron to HCl solutions reduced the anodic dissolution of Fe and delayed the hydrogen evolution reaction. The presence of Dipron either in MSD or NSD forms lowered both of I_{corr} and C_R of Fe electrode compared with obtained values of free HCl. Moreover, NSD form achieved lower I_{corr} and $C_R$values than MSD form. Also, increasing acid concentration resulted in decreasing IE% in the presence of the two forms of Dipron. Thus, at high acid concentration, the adsorbed inhibitor molecules could be expected to be desorbed by the retardation action of Cl^{-} ions (Attia and EL-Shafiey, 2009).

These results illustrated that adsorption of NSDform was stronger thanMSD form. The inhibition efficiency in presence of 10 mM of NSD reached its maximum value, 98.22 %, at 0.05M HCl, and it is higher than that of MSD which reached to 91.60 % at the same concentration. This might be owing to the presence of smaller nano particles of inhibitor in case of NSD form. However, as the size of a particle decreased, its surface area increased and also allowed a greater proportion of its atoms or molecules to be displayed on the surface rather than the bigger molecules (Nel*et al*., 2006).

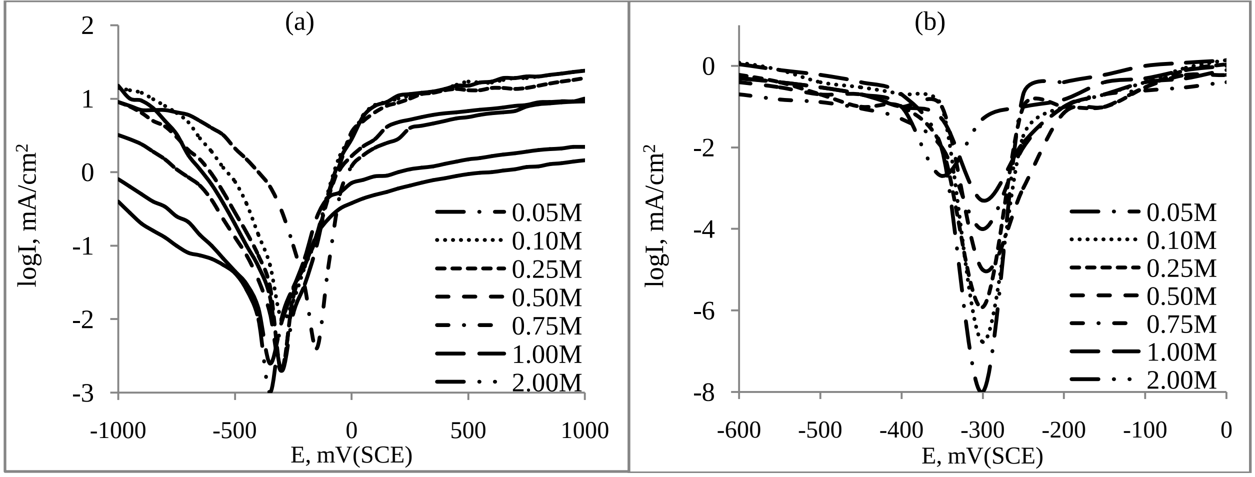

Fig 8: Potentiodynamic polarization plots of Fe in presence of 10 mM of Dipronsoluble in different concentrations of HCl solutions: (a) MSD, (b) NSD

Table 3:Potentiodynamicparameters of Fe in different concentrations of HCl solutions in presence of 10 mM of Dipron in MSD and NSD forms

Medium	C_{HCl} M	E_{corr} mV(SCE)	I_{corr} $\mu A/cm^2$	C_R mpy	b_a mV/dec	$-b_c$ mV/dec	IE%
10 mM MSD	0.05	-350	84	4	167	154	91.60
	0.10	-350	40	18	222	318	88.72
	0.25	-150	120	55	250	214	87.37
	0.50	-300	138	64	222	400	85.77
	0.75	-300	200	92	222	375	85.71
	1.00	-300	300	138	167	250	84.96
	2.00	-300	400	185	200	250	84.07
10 mM NSD	0.05	-350	2	0.82	75	50	98.22
	0.10	-300	8	3.69	50	50	97.74
	0.25	-300	30	13.8	40	31	96.84
	0.50	-300	40	18.4	182	29	95.88
	0.75	-300	68	31.4	20	31	95.14
	1.00	-300	100	46.1	21	17	94.98
	2.00	-300	250	115.4	11	18	90.05

The natural logarithms of C_R of Fe in absence and presence of 10 mM MSD and NSD versus the molar concentration of HCl (C_{HCl}) illustrated a straight line broken at approximately 0.25M HCl for all solutions. The following rate equation was set up to describe the straight line relationship (Attiaand Abdel- Salam, 2009).

$$\ln C_R = \ln K + \beta C_{HCl} \quad (10)$$

where$K$ is the specific corrosion reaction rate constant andβ is a constant for the reaction. Equation 10 is graphically shown in Figure 9 and the calculated kinetic parameters are listed in Table 4. It was clear that in the presence of both MSD and NSD forms, the magnitude of $C_R$was suppressed as its tendency to increase with increasing acid concentrations. This might be attributed to the suppression of Fe chloride by the adsorption of Dipron molecules (Attia and EL- Shafiey, 2009). The decrease of slope of the second part of broken lines might be arise from the formation of a tightly adsorbed, more protective Fe chloride compound on the metal at higher acid concentrations (> 0.25 M) (Attiaand Abdel- Salam, 2009). On the other hand, the presence of 10 mM of NSD soluble in different concentrations of HCl considerably decreased the magnitude of C_R compared with that of MSD. Values of β_1 and K_1in Table 4 represented the defined constants of equation 10at acid concentrations; 0.05, 0.10 and 0.25M HCl. On the other hand, values of β_2 and K_2 represented the same constants at acid concentrations of 0.50, 0.75, 1.00 and 2.00M

HCl. Data in Table 4 illustrated that, the constants β_1 and β_2 for inhibited solutions are higher than that for free HCl solutions. The rate constants of corrosion reaction, K_1 and K_2,decreasedin the following order:

Free HCl>MSD>NSD.

This indicated the inhibiting action of Dipron and the better action of NSD form.

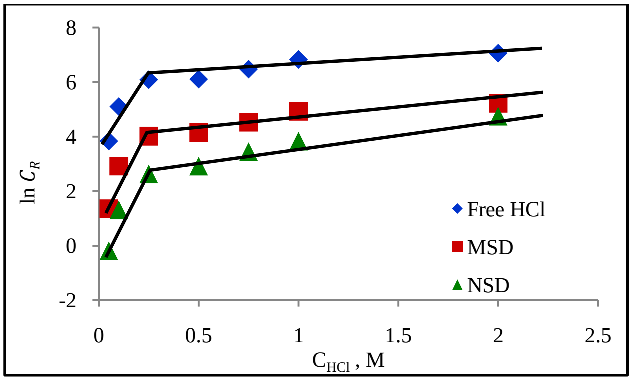

Fig 9: Variation of ln$C_R$ofFe with different concentrations of HClin absence and presence of 10 mM of Dipron in MSD and NSD forms at 25 °C.

Table 4: kinetic parameters for the corrosion of Fe in HCl solutions in absence and presence of 10 mM of Dipron in MSD and NSD forms

Medium	β_1	β_2	k_1	k_2
	mpy M		mpy	
Free HCl	25.33	0.59	1.30E-2	394
MSD	31.21	0.70	8.14E-4	51
NSD	30.06	1.21	1.83E-4	11

Effect of different concentrations of Dipronon corrosion behavior of Fe electrode

The effect of different concentrations of MSD and NSD on the potentiodynamic polarization of Fe was represented in Figure 10. It can be observed that the addition of different concentrations of NSD to 0.5M HCl shifted the anodic and cathodic branches of polarization curves of free acid solution towards lower current densities than MSD did. The potentiodynamic parameters of Dipron in the two forms were illustrated in Table 5. The values of I_{corr} and C_R decreased with increasing Dipronconcentration. This decrement indicated that addition of Dipronmolecules inhibited the corrosion process by decreasing the surface area for corrosion. This demonstrated that Dipron acted as inhibitor by adsorption onto Fe surface, and the inhibition degree depended on the nature of inhibitor and its concentration. Both b_a and b_c values changed noticeably in presence of the two forms of inhibitor than that observed in free acid solution. The inhibition efficiencies increased with increasing Dipronconcentration. The highest IE% of 97.9 occurred at 13.31 mMNSD compared with 89.7 for MSD. This was most likely due to the adsorption and formation of a good protective film by Dipron in MSD and NSD forms. The formation of a protective film was a result of the interaction of Dipronmolecules with atoms of the Fe surface. The smaller particles of NSD presented in HCl solution had high surface area that provided high reaction activities leading to an increase in the formation of a protective film (Awizar*et al.*, 2013).

Values of corrosion potential were not affected by addition of any concentration of MSD indicating that this form could act as pickling inhibitor, which in spite of leaving the corrosion potential virtually unaffected, caused a significant decrease in the corrosion rate (Attia and EL- Shafiey, 2009). The same behavior was recorded for NSD at concentrations 3.80, 9.50, 10.00 and 13.31 mM. On the other hand, a positive displacement of the E_{corr} values exhibited by 0.19 mMNSD was 200 mV(SCE) and by 0.95 and 1.90 mM was 100 mV(SCE). This meant that, at these concentrations, the dissolution of the anode could be controlled and the hydrogen evolution controlling process was reduced. An inhibitor can be classified as anodic or cathodic type when the change in E_{corr} value is higher than 85 mV in relation to that measured for the free solution (Pavithra*et al.*, 2013). Hence, it could be concluded that NSD form could act as pickling inhibitor at high concentrations and behaved as mixed type but predominantly anodic inhibitor at low concentrations.

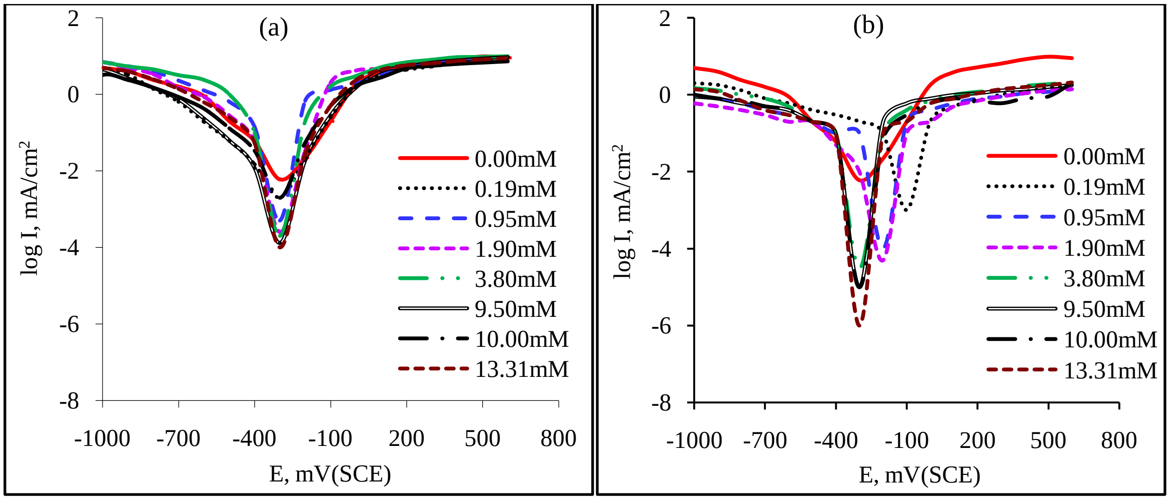

Fig 10: Potentiodynamic polarization plots of Fe electrode in different concentrations of Dipron in its two form: (a) MSD, (b) NSD.

Table 5: Potentiodynamic parameters of Fe in 0.5M HCl in absence and presence of different concentrations of MSD and NSD at 25 °C

Medium	C_{inh} mM	E_{corr} mV(SCE)	I_{corr} μA/cm^2	C_R mpy	b_a mV/dec	$-b_c$ mV/dec	IE%
Free HCl	0.00	-300	970	448	111	143	-
MSD	0.19	-300	316	146	185	200	67.4
	0.95	-300	200	92	100	160	79.4
	1.90	-300	180	83	100	200	81.4
	3.80	-300	160	74	100	100	83.5
	9.50	-300	145	67	133	171	85.0
	10.00	-300	140	64	222	400	85.6
	13.31	-300	100	46	142	250	89.7
NSD	0.19	-100	100	46	360	560	89.7
	0.95	-200	60	28	228	133	93.8
	1.90	-200	49	22	333	160	94.9
	3.80	-300	45	21	314	280	95.3
	9.50	-300	42	19	300	366	95.7
	10.00	-300	40	18	182	29	95.9
	13.31	-300	20	9	267	533	97.9

Adsorption isotherms:-

Freundlich isotherm:-

The Freundlich isotherm model was chosen to explain the adsorption of Dipronon the iron surface with uniform energy according to Eq. 11 (Erhayem*et al.*, 2015):

$$\theta = K_{ads} C_{inh}^{\frac{1}{n}} \quad (11)$$

The linearized form is given in Eq. 12:

$$\log\theta = \log K_{ads} + \frac{1}{n}\log C_{inh} \qquad (12)$$

where, K_{ads} (the equilibrium constant) and $\frac{1}{n}$ are indicators of the adsorption capacity and adsorption intensity respectively. $C_{inh}$is the inhibitor concentration (mM) and θ is the surface coverage degree. Figure (11-a) represented the adsorption of MSD and NSD on Fe surface according to this model. The adsorption parameters were listed in Table 6 and compared with that of Langmuir model.

It has been stated that the magnitude of $\frac{1}{n}$ gives an indication of the favorability and capacity of the adsorbent/adsorbate system. A value for $\frac{1}{n}< 1$ as in the present study indicated a normal Freundlich isotherm in which a significant adsorption took place at low concentration but the increase in the amount adsorbed with concentration became less significant at higher concentrations and vice versa, while $\frac{1}{n}> 1$ is indicative of cooperative adsorption (Attia and EL- Shafiey, 2009 and Teng and Hsieh, 1998). Also, the higher K_{ads} value for NSD indicates the greater the adsorption capacity. K_{ads} is related to the free energy of adsorption, ΔG°_{ads}, by Eq. 13:

$$K_{ads} = (1/55.5)\exp -\left(\Delta G^{\circ}_{ads}/RT\right) \qquad (13)$$

where 55.5 is the molar concentration of water, R is the universal gas constant and T is the absolute temperature.The obtained negative value of ΔG°_{ads} indicated that the adsorption process of Dipron in MSD and NSD forms on the Fe surface was spontaneous.

Langmuir isotherm:-

A mathematical representation of the Langmuir model was illustrated in Eq. 14 (Attia and EL- Shafiey, 2009 and Hussein *et al.*, 2014):

$$C_{inh}/\theta = 1/K_{ads}\,B_s + C_{inh}/B_s \quad (14)$$

where B_s, is the adsorbate binding capacity, that is, the maximum adsorption upon complete saturation of adsorbent surface.

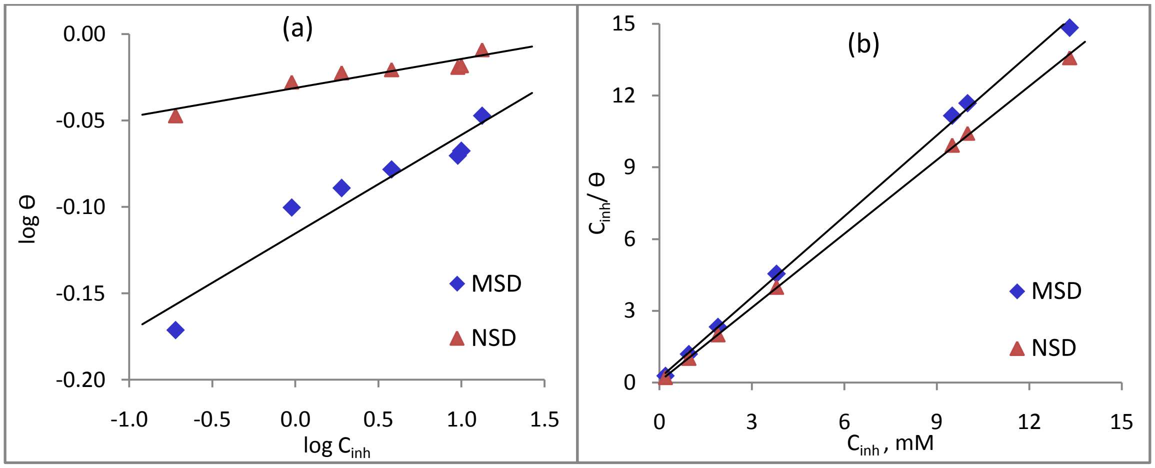

Fig 11: Adsorption isotherms of Dipron in MSD and NSD form on Fe surface: (a) Freundlich, (b) Langmuir.

Figure (11-b) and Table 6 showed that for Langmiure adsorption isotherm, the linear correlation coefficients (R^2) and the slopes of the two forms of Dipron were almost very close to unity, which indicated that the adsorption of Dipronin the micro and nano scale followed Langmuir adsorption isotherm. This meant that the solid surface contains a fixed number of adsorption sites and each site holds one adsorbed species (Abdul-Nabi and Jasim, 2013). The higher values of K_{ads} and B_s suggested higher capacity of the adsorption process and stability of the adsorbed layer on the Fe surface in the presence of NSD than that in presence of MSD. Values of ΔG°_{ads} between 0 and -20 kJ/mol, as in the present study, are consistent with spontaneous physical adsorption (Ansari *et al.*, 2014).

Table 6: Freundlich and Langmuir isotherms' constants for adsorption of Dipron in MSD and NSD forms on Fe surface at 25 °C

Isotherm parameters	MSD	NSD
Freundlich isotherm		
R^2	0.913	0.890
K_{ads}, mol^{-1}	0.766	0.931
n	17.513	59.523
$1/n$	0.057	0.017
ΔG°_{ads}, kJ/mol	-9.293	-9.773
Langmuire isotherm		
R^2	0.998	0.999
slope	1.128	1.027
B_s	0.886	0.973
K_{ads}, mol^{-1}	4.660	16.860
ΔG°_{ads}, kJ/mol	-13.765	-16.949

Effect of temperature on the corrosion behavior of Fe in 0.5M HCl in absence and presence of 10 mMof Dipron:-

Temperature is considered an important factor in the metal dissolution studies. The effect of temperature on the inhibition of metal corrosion reactions is very complex because different changes may occur on the metal surface such as rapid etching, desorption of inhibitor and the inhibitor may undergo decomposition (Karthik*et al*., 2015).

In this study, the effect of rising the temperature from 20 up till 60 °C on the corrosion behavior of Fe in free 0.5M HCl and in presence of 10 mM of Dipron inboth of MSD and NSD forms was studied. It was observed that variation of temperature had almost no effect on the general shape of the polarization curves as shown in Figure 12. Table 7 illustrated the effect of temperature on the corrosion potentials and corrosion rates of Fe in 0.5M HCl in absence and presence of 10 mM of Dipron inMSD and NSD forms and its corresponding inhibition efficiencies. By increasing the temperature, the corrosion rates increased and the free acid solution showed maximum corrosion rates than that in the presence of Dipron. This signified that the dissolution of the metal increased at higher temperatures indicating that the reactant molecules gained more energy and were able to overcome the energy barrier more rapidly. In addition, the present results also revealed that any increase in temperature caused increasing the solubility of the adsorbed films on the metals, thus increasing the susceptibility of the metal to corrosion which was in agreement with results reported by Sheeja and Subhashini (2014). The decrease in IE% with the increase in temperature might be attributed to the weakening of the physical adsorption process of inhibitor on the metal surface. For a physical adsorption mechanism, IE% of an inhibitor decreases with increasing temperature while for a chemical adsorption mechanism, values of inhibition efficiency increases with temperature (Sheeja and Subhashini, 2014).

It is noted from Table 7 that MSD had the best IE% value at 20 °C whereas the inhibition efficiency decreased at higher temperatures. On the other hand, NSD kept its tendency for inhibition efficiency constant even at higher temperatures owing to its greater activity which resulted from the presence of smaller nano particle size in the corrosive HCl solution.

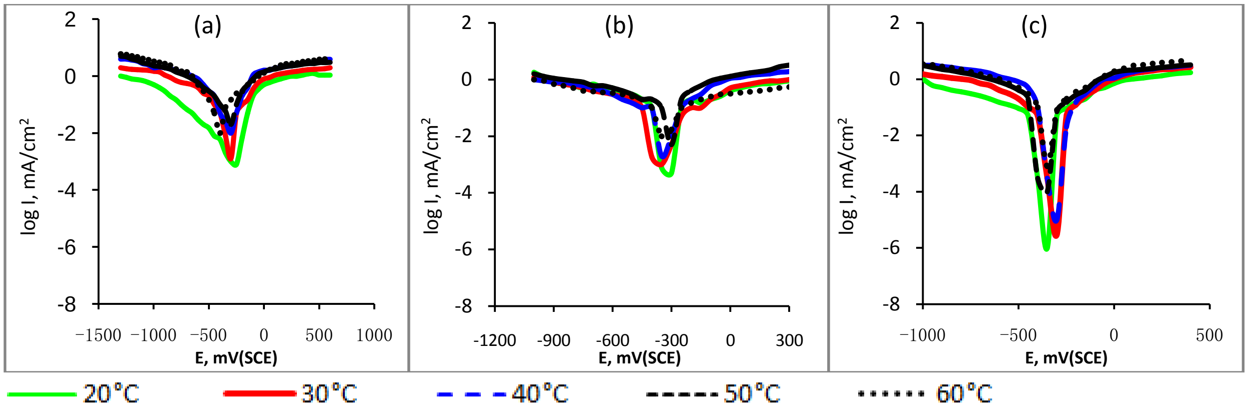

Fig 12: Effect of temperature on potentiodynamic polarization of Fe electrode in 0.5M HCl in absence and presence of 10 mM of Dipron: (a) free HCl (b) MSD (c) NSD.

Table 7: Corrosion potential and corrosion rates of Fe electrode in 0.5M HCl in absence and presence of 10 mM of Dipron inMSD and NSD forms and the corresponding inhibition efficiencies at different temperatures

	Free HCl		MSD			NSD		
T °C	E_{corr} mV(SCE)	C_R mpy	E_{corr} mV(SCE)	C_R mpy	IE%	E_{corr} mV(SCE)	C_R mpy	IE%
20	-250	369	-300	23.1	93.75	-350	6.9	98.13
30	-300	453	-350	64.7	85.71	-300	18.9	95.82
40	-300	508	-350	73.9	85.45	-300	22.2	95.64
50	-300	647	-300	97.9	84.85	-350	28.6	95.57
60	-400	785	-350	161.6	79.41	-350	35.1	95.53

The dependence of corrosion rate (C_R) on temperature can be expressed by the Arrhenius equation (Karthik *et al.*, 2015):

$$\log C_R = A - (E_a/2.303\, RT) \quad (15)$$

where A is a constant representing the frequency factor, E_a is the apparent activation energy of the Fe dissolution reaction, R is the universal gas constant and T is the absolute temperature. Values of E_a can be calculated from the slopes of the straight line obtained by plotting $\log C_R$ vs $1/T$ as illustrated in Figure 13(a). The thermodynamic functions for dissolution of Fe in 0.5M HCl in absence and presence of 10 mMDipron in MSD and NSD forms were obtained by applying the Eyring transition-state equation (Eq. 16) (Abdul-Nabi and Jasim, 2013 and Karthik*et al.*, 2015):

$$\log C_R/T = \log(R/Nh) + (\Delta S^\circ/2.303R) - (\Delta H^\circ/2.303RT) \qquad (16)$$

where$N$ is Avogadro's number, h is Planck's constant, ΔS° and $\Delta H^\circ$are the entropy and enthalpy of activation, respectively.A plot of $\log C_R/T$ vs. $1/T$ gave straight line with slope of$[-\Delta H^\circ/2.303R]$andan intercept of $[\log(R/Nh) + (\Delta S^\circ/2.303R)]$as illustrated in Figure 13(b).The obtained values were tabulated in Table 8.

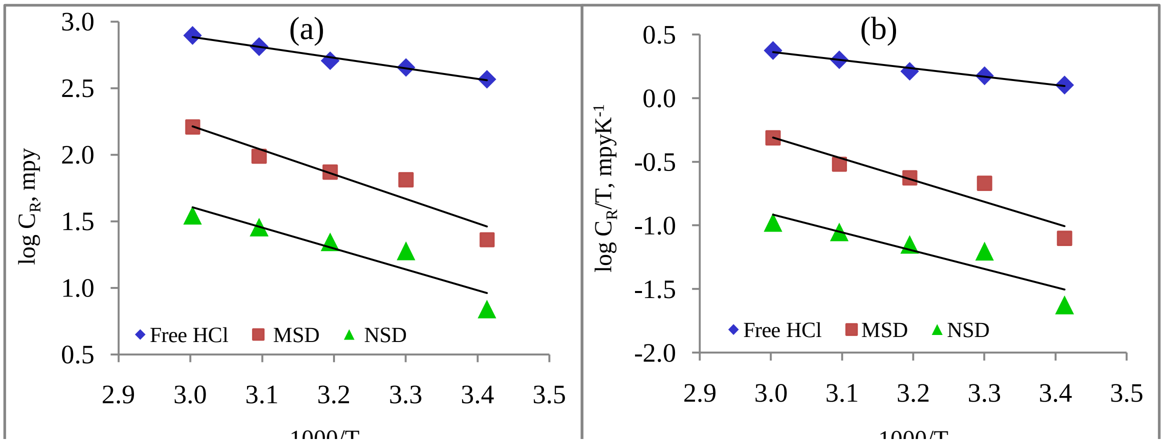

Fig 13: (a) Arrhenius plot,(b) Transition state plot.

Table 8: Activation parameters of Fe in 0.5M HCl in absence and presence of 10 mM of Dipron

Medium	E_a kJ/mol	ΔH° kJ/mol	ΔS° J/mol K
Free HCl	15	12	-153
MSD	35	32	-106
NSD	30	27	-133

The increase in$E_a$andΔH° in the presence of MSD and NSD forms implied that addition of Dipronto the acid solution increased the height of the energy barrier of the corrosion reaction and indicated that as the temperature was raised a decrease in protection efficiency was obtained (Fouda*et al*., 2010). It was noted from Table 8 that E_a for the corrosion process, in presence of Dipron, was greater than 20 kJ/moland hence the entire process was controlled by surface reaction (Fouda*et al*., 2009). Based on the temperature effects, Priya*et al*. (2008) classified the relationships between the temperature dependence of IE%of an inhibitor and the E_a, into three groups: i) IE%decreases with the increase in temperature: E_a(inhibited solution) >E_a(uninhibited solution); ii) IE%increases with the increase in temperature: E_a(inhibited solution) <E_a(uninhibited solution) and iii) IE%does not change with temperature: E_a(inhibited solution) = E_a(uninhibited solution).

From the obtained findings, according to Tables 7 and 8, group (i) was the applied case in which the values of $E_a$suggests the physisorption mechanism. The positive signs of ΔH° reflected the endothermic nature of Fe dissolution process which suggested its difficult and slow dissolution in presence of Dipron in MSD and NSD forms. Values of entropy of activation (ΔS°) illustrated less negativity for inhibited solutions than that for the uninhibited one. This implied that the activated complex represented an association rather than a disordering going from reactants to the activated complex (Abdul-Nabi and Jasim, 2013). This reflected the formation of an ordered stable layer of inhibitor on the Fe surface (Al-Bonayan, 2015). Thus, it could be confirmed that the nature of inhibitor and the temperature of solution affected greatly the activation parameters of the corrosion process.

Potentiostatic polarization:-

Effect of applied potential:-

Figure 14(a, b and c) showed the variation of current density with time at different applied potentials (E_A) for Fe electrode in 0.5M HCl in absence and presence of 10 mM of Dipron in MSD and NSD forms, respectively. The corresponding values of initial current density (i_i), stabilized current density (i_s),quantity of electricity (Q) and surface charging capacity (C) were summarized in Table 9. It was clear that, for each type of solution, as a general trend, the i_i, i_s and Q increased by increasing the applied potentials. Comparing the three types of solutions, values of i_i, i_s, Q and C for Fe electrode generally decreased in the following order: Free HCl > MSD > NSD

This illustrated the effective action of Dipron in MSD and NSD forms on the corrosion inhibition of Fe in 0.5M HCl and ensured the better action of NSD form. These results were in good agreement with those obtained in OCP and potentiodynamic polarization measurements.

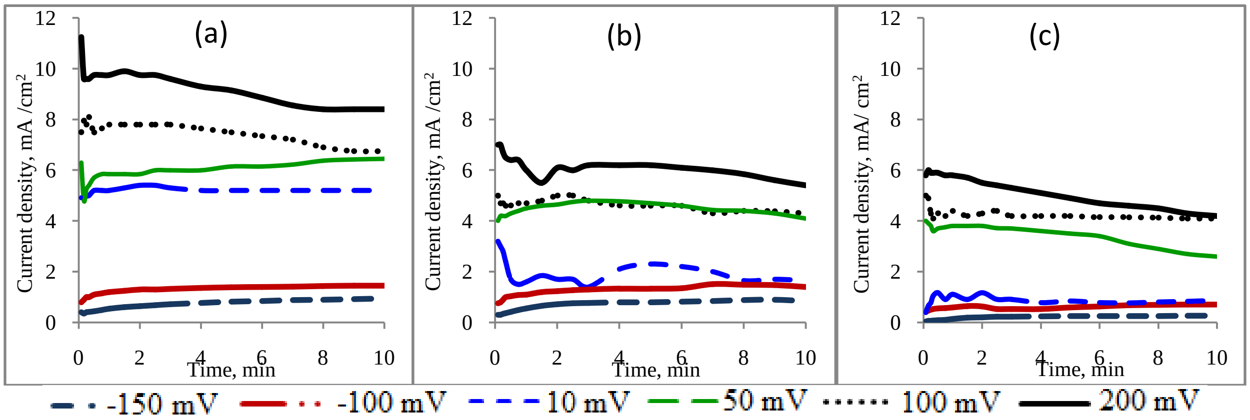

Fig 14: Potentiostatic polarization plots of Fe electrode at different applied potentials in 0.5M HCl in absence and presence of 10 mM of Dipron: (a) free HCl (b) MSD (c) NSD.

Table 9: Potentiostatic parameters of Fe in 0.5M HCl in absence and presence of 10 mM of Dipron in MSD and NSD forms at different applied potentials at 25 °C

Medium	E_A mV(SCE)	i_i mA/cm^2	i_s mA/cm^2	Q mC/cm^2	C mF/cm^2
Free HCl	-150	0.40	0.95	85	0.57
	-100	0.80	1.45	130	1.31
	10	4.91	5.20	1092	109.20
	50	6.30	6.45	290	5.81
	100	7.50	6.75	1012	10.12
	200	11.25	8.40	1008	5.04
MSD	-150	0.30	0.85	76	0.51
	-100	0.75	1.40	84	0.84
	10	3.20	1.65	198	19.80
	50	4.00	4.10	184	3.69
	100	5.00	4.30	645	6.45
	200	7.00	5.40	972	4.86
NSD	-150	0.04	0.26	24	0.16
	-100	0.41	0.71	42	0.42
	10	0.39	0.87	157	15.68
	50	4.00	2.60	156	3.12
	100	5.00	4.10	615	6.15
	200	5.80	4.20	630	3.15

The highest Q values observed for free 0.5M HCl were due to the preferential adsorption of Cl^- ions on the oxide surface acting as a depolarizer for the main anodic process of oxygen discharge (Attia, 2006). The results showed that the surface charging capacity reached its maximum value at 10 mV(SCE) in the three types of solutions.

Effect of inhibitor concentration:-

Figure 15 and Table 10 illustrated the effect of Dipron concentration at constant applied voltage of 10 mV(SCE) on the potentiostatic behavior of Fe in 0.5M HCl at 25 °C. It was clearly observed that the presence of different concentrations of Dipron in MSD and NSD forms was accompanied by a reduction in stabilized current density compared with that recorded for free acid solution. The current densities decreased with increasing inhibitor concentrations. This was an indicative of passivation of the electrode in the presence of the two forms of Dipron. The decrease in C values in the presence of inhibitor was attributed to a decrease in active sites because of the adsorbed Dipron in micro and nano scale particle size (Kumar and Venkatesha, 2013). The values of film thickness

(d) did not change regularly with the Dipron concentration. But in all cases, it was higher in the presence of Dipron than that of free acid solution, and in most cases it was higher in the presence of NSD compared with MSD indicating its better protective properties. It is worthy to mention that 10 mM of Dipron concentration showed better protective properties than other concentrations and could be considered as an optimum concentration for this study. This result was in good agreement with that obtained in OCP measurements.

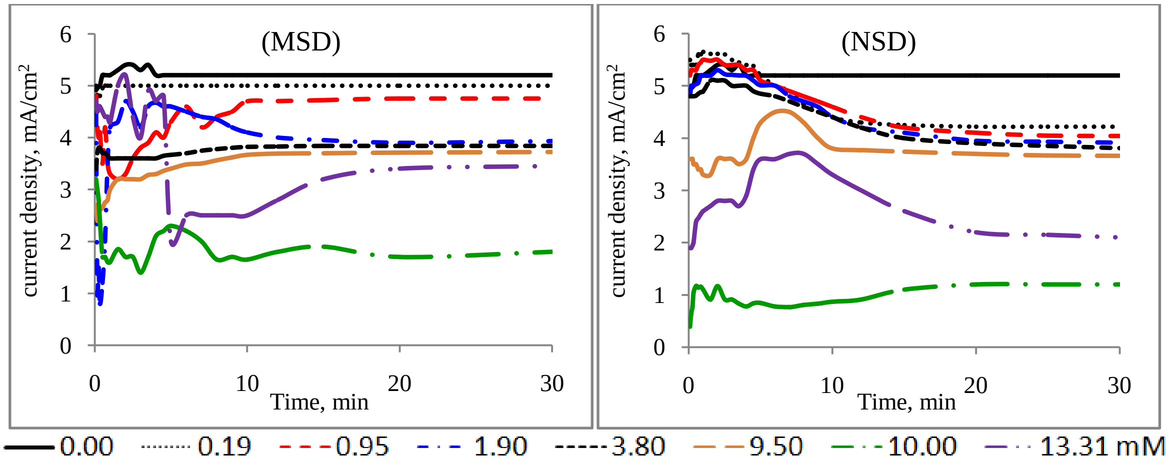

Fig 15: Potentiostatic polarization plots of Fe in 0.5M HCl in absence and presence of different concentrations of Dipron at constant applied voltage of 10 mV(SCE).

Table 10: Potentiostatic parameters of Fe in 0.5M HCl in absence and presence of different concentrations of Dipron at constant applied voltage of 10 mV(SCE) at 25 °C

	MSD				NSD			
C_{inh}mM	i_i mA/cm^2	i_s mA/cm^2	C mF/cm^2	d Å$*10^{-6}$	i_i mA/cm^2	i_s mA/cm^2	C mF/cm^2	d Å$*10^{-6}$
0.00	4.91	5.20	109.20	1.89	4.91	5.20	109.20	1.89
0.19	5.00	5.00	60.00	3.45	5.50	4.22	25.32	8.17
0.95	4.80	4.75	57.00	3.63	5.20	4.04	24.24	8.54
1.90	4.50	3.93	82.53	2.51	4.80	3.91	19.54	10.59
3.80	3.40	3.84	80.64	2.56	4.80	3.81	45.72	4.53
9.50	2.70	3.72	78.12	2.65	3.60	3.66	76.86	2.69
10.00	3.20	1.80	86.40	2.40	0.39	1.20	21.60	9.58
13.31	4.70	3.45	103.50	2.00	1.90	2.10	37.80	5.47

Effect of temperature:-

Figure 16 represented the temperature effect on corrosion behavior of Fe electrode immersed in 0.5M HCl in absence and presence of 10 mM of Dipron in MSD and NSD forms at constant applied voltage of 10 mV(SCE). The potentiostatic parameters were tabulated in Table 11. It was clear that, for the three types of solutions, i_i, i_s, $Q$and C, all generally increased with increasing temperature obeying the following order:FreeHCl>MSD>NSD. This could be attributed to an appreciable decrease in the adsorption of Dipron on the Fe surface with increase in temperature and a corresponding increase in corrosion rates expected due to the fact that greater area of metal was exposed to acid environment. The reciprocal capacitances which represent the film stability were always having higher values for acid solutions containing NSD than that containing MSD at all temperatures. From Figure 16 and Table 11, it could be concluded that the presence of Dipron in its two forms inhibited the corrosion of Fe in 0.5M HCl. Also, the presence of NSD in 0.5M HCl solution resisted the increasing Fe corrosion accompanied by increasing temperature more effectively than MSD did.

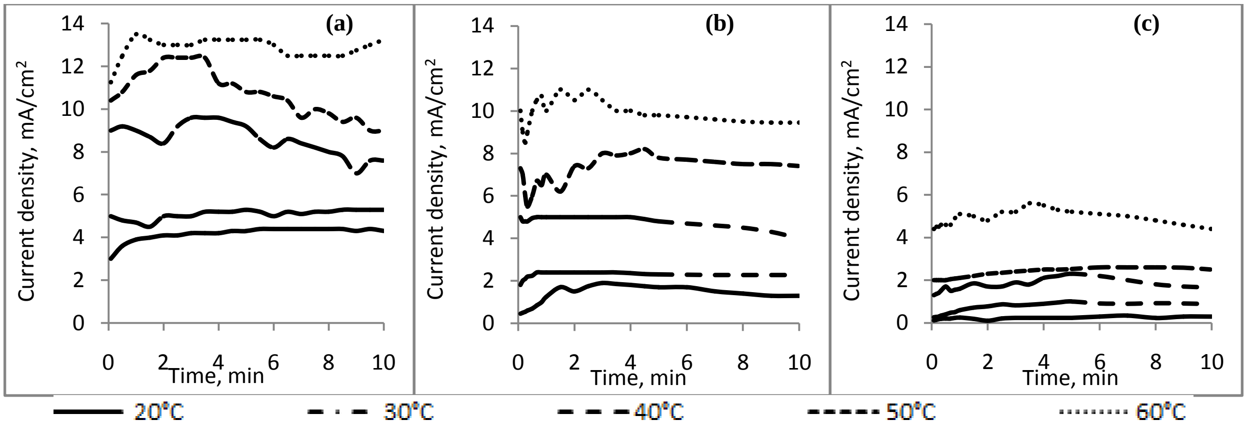

Fig 16: Effect of temperature on Fe electrode at constant applied voltage of 10 mV(SCE) in 0.5M HCl in absence and presence of 10 mM of Dipron: (a) free HCl (b) MSD (c) NSD.

Table 11: Potentiostatic parameters of Fe electrode in 0.5M HCl in absence and presence of 10 mM of Dipron in MSD and NSD forms at constant applied voltage of 10 mV(SCE) at different temperatures

Medium	Temp. °C	i_i mA/cm^2	i_s mA/cm^2	Q mC/cm^2	C mF/cm^2	C^{-1} cm^2/mF
Free HCl	20	3.00	4.30	258	25.80	3.88E-02
	30	5.00	5.30	636	63.60	1.57E-02
	40	9.00	7.60	912	91.20	1.10E-02
	50	10.40	9.00	270	27.00	3.70E-02
	60	11.25	13.25	795	79.50	1.26E-02
MSD	20	0.45	1.30	156	15.60	6.40E-02
	30	1.80	2.27	204	20.43	4.89E-02
	40	5.00	4.00	480	48.00	2.08E-02
	50	7.30	7.40	1332	133.20	7.51E-03
	60	10.00	9.45	1984	198.45	5.04E-03
NSD	20	0.12	0.30	36	3.60	2.78E-01
	30	0.27	0.88	158	15.80	6.31E-02
	40	1.30	1.65	346	34.65	2.89E-02
	50	2.00	2.50	375	37.50	2.67E-02
	60	4.40	4.40	924	92.40	1.08E-02

The inhibition mechanism:-

In hydrochloric acid medium, the Fe surface was negatively charged due to the specifically adsorbed chloride ions on the surface. Owing to the acidity of the medium, the –NH_2 group in Dipron could not remain in solution as free base. It exists as a neutral species or in the cationic form as indicated below. Also, the oxygen and sulfure atoms in the sulfamidic group can be protonated easily, due to high electron density on it, leading to positively charged inhibitor species. Thus, Dipron inhibitor may adsorb through the electrostatic interactions between the positively charged Dipron molecules and the negatively charged Fe surface. Moreover, the adsorption of Dipron molecules could also be occurred due to the formation of links between the d-orbital of Fe atoms, involving the displacement of water molecules from the metal surface, and the lonely sp^2 electron pairs present on the N and O atoms of the sulfamidic group (El-Naggar, 2007).

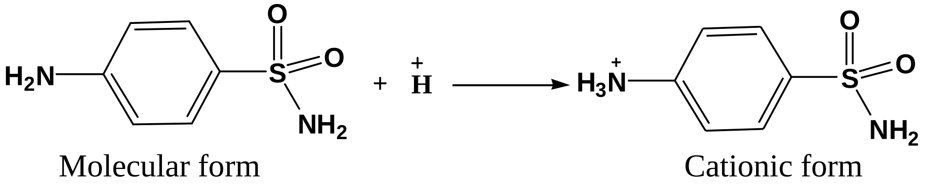

Conclusions:-

1. From OCP, potentiodynamic and potentiostatic polarization measurements, the corrosion of Fe in HCl solutions was retarded in the presence of Dipron in MSD and NSD forms and the effect of NSD was more pronounced than MSD.
2. Dipron in MSD form could act as pickling inhibitor, while in NSD form could act as pickling inhibitor at high concentrations and behaves as mixed type but predominantly anodic inhibitor at low concentrations.
3. The inhibition efficiency increased with increasing Dipron concentration but decreased with increasing acid concentration and solution temperature.
4. 10 mM of Dipron was considered as optimum concentration for corrosion inhibition of Fe in 0.5M HCl solution.
5. The inhibition effect and corrosion protection increased as the particle size of inhibitor decreased even in small percentage in heterogeneous system.

References:-

1. Abdel Hameed, R.S. (2011): Ranitidine drugs as non-toxic corrosion inhibitors for mild steel in hydrochloric acid medium. Port. Electrochim. Acta, 29(4): 273-285.
2. Abdul-Nabi, A.S. and Jasim, E.Q. (2013): Synthesis, characterization of some azo dyes derived from sulfa drugs and the use of them as corrosion inhibitors in 0.5 M hydrochloric acid solution. J. Basrah. Res. (Sci.), 39(3): 82-106.
3. Al-Bonayan, A.M. (2015): Corrosion inhibition of carbon steel in hydrochloric acid solution by Senna-Italica extract. IJRRAS., 22(2): 49-64.
4. Ansari, A., Znini, M., Hamdani, I., Majidi, L., Bouyanzer, A. and Hammouti, B. (2014): Experimental and theoretical investigations anti-corrosive properties of Menthone on mild steel corrosion in hydrochloric acid. J. Mater. Environ. Sci., 5(1): 81-94.
5. Arslan, T., Kandemirli, F., Ebenso, E.E., Love, I. and Alemu, H. (2009): Quantum chemical studies on the corrosion inhibition of some sulphonamides on mild steel in acidic medium. Corros. Sci., 51: 35-47.
6. Attia, E.M. (2006): Electrochemical behavior of titanium electrode in aqueous bromide solutions. Al-Azhar Bull. Sci., 17(2): 53-71.
7. Attia, E.M. (2015): Expired Farcolin drug as corrosion inhibitor for carbon steel in 1M HCl solution. J. Basic. Appl. Chem., 5(1): 1-15.
8. Attia, E.M. and Abdel- Salam, F.H. (2009): The effect of triazolethione derivative on the corrosion of Fe in hydrochloric acid solutions. Al-Azhar Bull. Sci., 20(2): 43-58.
9. Attia, E.M. and EL- Shafiey, Z.A. (2009): Inhibition of Fe corrosion using two newly synthesized Schiff base complexes in ethanolic hydrochloric acid media. Al-Azhar Bull. Sci., 20(2): 23-42.
10. Awizar, D.A., Othman, N.K., Jalar, A., Daudv, A., Abdul Rahman, I. and Al-hardan, N.H. (2013): Nanosilicate extraction from rice husk ash as green corrosion inhibitor. Int. J. Electrochem. Sci., 8: 1759 – 1769.
11. Balonis, M. (2010): The influence of inorganic chemical accelerators and corrosion inhibitors on the mineralogy of hydrated Portland cement systems. Ph.D Thesis, Department of Chemistry, University of Aberdeen, United Kingdom.
12. Ebenso, E.E., Eddy, N.O. and Odiongenyi, A.O. (2009): Corrosion inhibition and adsorption properties of methocarbamol on mild steel in acidic medium. Port. Electrochim. Acta, 27(1): 13-22.
13. El-Naggar, M.M. (2007): Corrosion inhibition of mild steel in acidic medium by some sulfa drugs compounds. Corros. Sci., 49: 2226-2236.
14. Erhayem, M., Al-Tohami, F., Mohamed, R. and Ahmida, K. (2015): Isotherm, kinetic and thermodynamic studies for the sorption of mercury (II) onto activated carbon from rosmarinusofficinalis leaves. Am. J. of Analy. Chem., 6: 1-10.
15. Fouda, A.S., Heakal, F.E. and Radwan, M.S. (2009): Role of some thiadiazole derivatives as inhibitors for the corrosion of C-steel in 1 M H_2SO_4. J. Appl. Electrochem., 39(3): 391-402.
16. Fouda, A.S., Mostafa, H.A. and El-Abbasy, H.M. (2010): Antibacterial drugs as inhibitors for the corrosion of stainless steel type 304 in HCl solution. J. Appl. Electrochem., 40(1): 163-173.
17. Hussein, W.A.M., Attia, E.M., Ghayad, I.M. and Ghanem, W.A.M. (2014): Electrochemical behavior and corrosion inhibition of zinc electrode in solutions of $(NH_4)_2SO_4$ containing Ce (IV) ions. Researcher, 6(1): 1-11.

18. Karthik, R., Muthukrishnan, P., Chen, S.M, Jeyaprabha, B. and Prakash, P. (2015): Anti-corrosion inhibition of mild steel in 1 M hydrochloric acid solution by using Tiliacoraaccuminata leaves extract. Int. J. Electrochem. Sci., 10: 3707-3725.
19. Kumar, M.K.P. and Venkatesha, T.V. (2013): Fabrication of zinc-nano TiO_2 composite films: Electrochemical corrosion studies. J. Chem. Pharm. Res., 5(5): 253-261.
20. Nel, A., Xia, T., Mädler, L. and Li, N. (2006): Toxic potential of materials at the nanolevel. Science, 311: 622-627.
21. Pathak, R.K. (2013): Electrosynthesis and characterization of CdSeHgTl thin films. RJCS., 3(4): 44-47.
22. Pavithra, M.K., Venkatesha, T.V. and Punith Kumar, M.K. (2013): Inhibiting effects of Rabeprazole sulfide on the corrosion of mild steel in acidic chloride solution. Int. J. Electrochem., 2013: 1-9.
23. Pourbaix, M. (1974): Atlas of electrochemical equilibria in aqueous solutions, 2nd Ed., NACE, Houston, TX, USA, P. 307.
24. Priya, A.R.S., Muralidharam, V.S. and Subramania, A. (2008): Development of novel acidizing inhibitors for carbon steel corrosion in 15% boiling hydrochloric acid. Corrosion, 64(6): 541-552.
25. Quraishi, M.A., Sudheer and Ebenso, E.E. (2012): Ketorol: New and effective corrosion inhibitor for mild steel in hydrochloric acid solution. Int. J. Electrochem. Sci., 7: 9920-9932.
26. Selvakumar, P., Karthik, B.B. and Thangavelu, C. (2013): Corrosion inhibition study of stainless steel in acidic medium – An overview. Res. J. Chem. Sci., 3(4): 87-95.
27. Sheeja, V.N. andSubhashini, S. (2014): Pavettaindica bark as corrosion inhibitor in mild steel corrosion in HCl and H_2SO_4 medium: Adsorption and thermodynamic study. Chem. Sci. Trans., 3(1): 129-140.
28. Teng, H. and Hsieh, C. (1998): Influence of surface characteristics on liquid-phase adsorption of phenol by activated carbons prepared from bituminous coal. Ind. Eng. Chem. Res., 37: 3618-3624.